

# Effect of Mass Flow and Mold Temperature in the Mechanical Properties of Polypropylene-rice Rusk Ash

Duarte, G. W.<sup>\*1</sup>, Fiori, J. Jr.<sup>1</sup>, Peterson, M.<sup>1</sup>, Fiori, M. A.<sup>1</sup>, Colle, G. N.<sup>2</sup>, Riella, H. G.<sup>2</sup>, Neto, A. B. S. S.<sup>3</sup>

<sup>1</sup>Programa de Pós-Graduação em Ciências e Engenharia de Materiais, Universidade do Extremo Sul Catarinense - UNESC - 88806-000, Criciúma, SC, Brazil

<sup>2</sup>Programa de Pós-Graduação em Engenharia Química, Universidade Federal de Santa Catarina – UFSC, Florianópolis, SC, Brazil

<sup>3</sup>Programa de Pós-Graduação em Engenharia, Universidade Federal do Pampa, UNIPAMPA, Bagé RS, Brazil

\*gwduarte@gmail.com

**Abstract-** This work aims to study the influence of mass flow and mold temperature in the mechanical properties of RHA/PP composites using, as parameter, the crystallinity degree of the composite. The samples were obtained following a statistical experimental factorial planning, in which it was ranged the mass flow and mold temperature. The samples underwent tensile and bending tests, DSC and SEM in order to verify the mechanical and morphological properties. The results of mold temperature showed significance in the crystallinity degree of the composite matrix. And both mold temperature and mass flow are significant for the mechanical properties of the composite.

**Keywords-** Rice Husk Ash; Polymer Composite; Mechanical Properties; Injection Parameters; Statistical Experimental Factorial Planning

## I. INTRODUCTION

The materials processing industry increasingly seeks to improve its production and enable the manufacture of its products with the use of new materials or low-cost formulations, for example, with the use of rejects from manufacturing processes.

One of the wastes that have aroused great interest in the industry is the rice husk ash (RHA). Globally, about 120 million tons of rice husk ash is produced each year and, its disposable is considered a serious problem for the producers due to the large amount that accumulates in the vicinity of rice mills [1]. Rice Husk Ash has been used as an additive for concrete and cement [2-6], as adsorbents for Hg species [7, 8], SO<sub>2</sub> [9, 10], CO<sub>2</sub> [11] and other metals in biodiesel [12], for the production of geopolymers [13, 14] and pigments for ceramics [15].

The rice husk ash is also applied in development and research with polymers. The RHA has been used as additives in rubbers and silicones studies [16-19] and to improve the properties of mechanical wear of PVC [20]. Many studies are concerned of applying the RHAs as elements of polymer matrix composites and evaluating the effect of addition of RHA in the mechanical properties and morphological characteristics of RHA-RHA-Polypropylene and polyethylene composites [21-28]. G. C. Nascimento et al. studied the effect of the percentage of RHA and its particle size in the mechanical properties of the composite RHA/PP. They proved that both weight percentages of RHA particle size promote a decrease of the Tensile Strength, but do not affect its tenacity. So, with appropriate combinations of the variables studied it is possible to produce a composite with good mechanical properties [29].

In particular, polypropylene is one of the most widely used industrial polymers, with applications in automotive, electrical appliances, packaging and in other medical products and offers great scope to fabricate composite of the type RHA/PP. The research works with RHA/polymer composite have been carried out with emphasis on the mechanical properties, with evaluation of the effect of different types of compatibilizer agents, different additives or different compositions. However, for technological applications it is also important to evaluate the processability of these materials as well as the effect of processing variables on its properties. For homogenization and processing of the pellets it typically employed the technique of extrusion. But, as most of manufacture process leads to the injection of the final products it is important to evaluate the effect of the processing parameters for this technique.

Therefore, this paper presents results of investigations carried out with polypropylene-rice husk ash (RHA/PP) composite processed by extrusion and injection, evaluating the effect of injection processing variables such as mass flow and the mold temperature on the mechanical properties and crystallinity degree of RHA/PP composites.

## II. EXPERIMENTAL

### A. Processing of RHA/PP Composite

It was used, as polymeric matrix, polypropylene from BRASKEN S.A. and, as composite element, the rice husk ash (RHA)

with a mean particle size of 6.0  $\mu\text{m}$ . The evaluated formulation was 95.0 wt% polypropylene and 5.0 wt% of RHA for all the experiments. The formulation of the rice husk ash/polypropylene (RHA/PP) was prepared and homogenized in a single screw extruder ORIZON, OZ-E-EX-t22, with L/D = 17.

The extruder has four zones with controlled temperature. The setting for these zones was:  $Z_1 = 165.0^\circ\text{C}$ ,  $Z_2 = 175.0^\circ\text{C}$ ,  $Z_3 = 185.0^\circ\text{C}$  and  $Z_4 = 185.0^\circ\text{C}$ . The screw velocity used was 55 rpm.

In these conditions the pellets of RHA/PP composite were obtained and they were stored in appropriate packages avoiding light and humidity. Before the injection processing, the RHA/PP pellets were dried in an oven with temperature of  $(60.0 \pm 1.0)^\circ\text{C}$  for 24 hours.

### B. Injection of the Samples of RHA/PP

The injection processing of RHA/PP pellets was performed in an injector HIMACO, model LHS 150-80. The injection has four zones of controlled temperature. The setting of the zones was:  $Z_1 = 165.0^\circ\text{C}$ ,  $Z_2 = 175.0^\circ\text{C}$ ,  $Z_3 = 175.0^\circ\text{C}$  and  $Z_4 = 85\%$ . Where the 85% corresponds to the percentage of time during which the thermistor keeps on.

The injection mold temperature was set and kept constant by a thermo-stable bath system coupled to the injector. The thermal stabilizer is from MICROQU MICA, model MQBMP-01 and uses water as the refrigerant fluid. The thermal stabilizer system was put in operation four hours before the injection procedures to guarantee the stabilization of the mold temperature. The geometry of the samples of RHA/PP followed the ABNT NBR 9622:1986.

### C. Characterization of the Samples of RHA/PP

The tensile tests were performed according to ABNT NBR 9622:1986, using a universal mechanical testing machine, EMIC, model DL 20000 N, with velocity of 10.0 mm/min, load cell of 500.0 kgf and electronic extensometer coupled.

For the flexural tests the methodology described at ASTM 790:92, procedure B, was followed. The velocity was 16.0 mm/min in a universal mechanical testing machine, EMIC, model DL 20000 N, coupled with a load cell of 50.0 kgf and electronic deflectionometer.

In order to verify the crystallinity degree it employed the technique of DSC (*Differential Scanning Calorimetry*). The equipment used was a DSC system from TA INSTRUMENTS, model Q200, with a rate of heating/cooling of 10.0  $^\circ\text{C}/\text{min}$ .; being the cooling controlled by cryogen.

The micrographs were obtained by scanning electron microscope (SEM) with a PHILLIPS equipment, model XL 30, equipped with microprobe energy dispersive x-ray (EDX) from EDAX. The samples analyzed were the ones which were broken at the tensile tests. To make the surface become conductive, gold was deposited on the surface and a foil strip laterally for the ohmic contact with the support of the samples.

## III. RESULTS AND DISCUSSION

In this work it used an experimental factorial planning  $2^2$ , with three central points. The variables evaluated were the mold temperature and mass flow in the mechanical properties of RHA/PP composites. The minimum, central and maximum values for the mold temperature were 18.0  $^\circ\text{C}$ , 43.5  $^\circ\text{C}$  and 69.0  $^\circ\text{C}$ , respectively. For the mass flow, the minimum and maximum values were 4.0 and 21.0 g/s, respectively, and the central value was 15.0 g/s.

Fig. 1 shows the comparison between the thermograms for the samples of RHA/PP obtained with mass flow of 4.0 g/s and mold temperature of 18.0  $^\circ\text{C}$  and 69.0  $^\circ\text{C}$ . The thermograms indicate that melt temperature is 132.0  $^\circ\text{C}$  and it is not affected by mold temperature variation, thus indicating that the crystalline structure of the polymer phase is not affected.

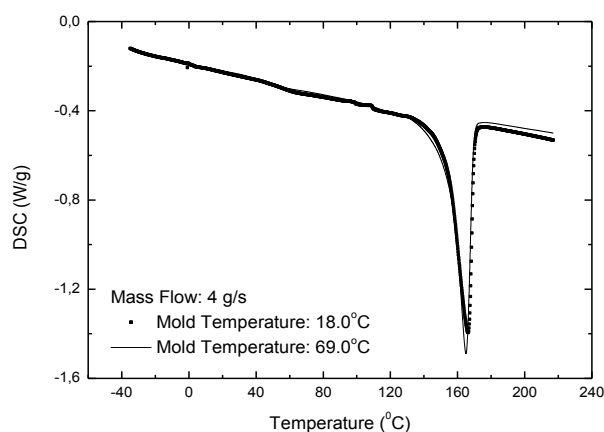


Fig. 1 DSC Thermograms for the samples of RHA/PP produced with mass flow of 4.0 g/s and different mold temperature

In the transition region between 132.0 °C and 179 °C the thermograms demonstrate endothermic peak transition with different values of area, Fig. 2. The values of area are directly related with the amount of energy absorbed by the RHA/PP composite to achieve complete fusion of the crystalline phases of the polymeric matrix. As is observed in the thermogram, the samples prepared with higher mold temperatures have peaks with larger area, so it is possible to conclude that higher mold temperature provides higher crystallinity degree of the polymeric matrix. The value for the crystallinity degree is 30.8% for samples produced with mold temperature of 18.0 °C and 34.0% for the samples produced with mold temperature of 69.0 °C.

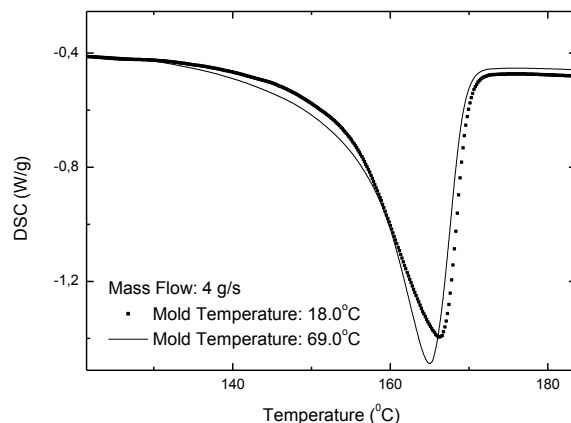


Fig. 2 Difference between peaks related with melting transition of crystalline phase of the polymeric matrix of composite for the samples produced with mass flow of 4.0 g/s and different mold temperature

Table 1 shows the values of crystallinity degree determined by DSC thermograms for the samples of RHA/PP composite, processed with different mold temperatures and different mass flow. The results indicate that the increase of the mold temperature promotes a variation in the crystallinity degree of about 3.0%, while the variation of crystallinity degree with the mass flow is apparently not significant.

TABLE 1 MATRIX OF RESPONSE FOR THE CRYSTALLINITY DEGREE

Experiment	Mass flow [g/s]	Mold Temperature [°C]	Xc (%)
1	4.0	18.0	30,8
2	21.0	69.0	34,4
3	21.0	18.0	31,4
4	4.0	69.0	34,0
5	15.0	43.5	32,4
6	15.0	43.5	32,3
7	15.0	43.5	31,9

The analysis of variance (ANOVA) shows that mold temperature is a statistically significant factor in RHA/PP crystallinity degree, while the mass flow does not present significance in a 95.0% reliability degree, showed in Table 2. From estimated effects matrix in Table 3, it is possible to verify that the mold temperature affects the crystallinity degree with a positive effect with an order of  $3.10000 \pm 0.26458$ .

TABLE 2 ANOVA FOR CRYSTALLINITY DEGREE

	SS	df	MS	F	P
Mass flow	0,14408	1	0,144083	2,0583	0,287830
*Mold Temperature	9,61000	1	9,610000	137,2857	0,007205
1 by 2	0,01000	1	0,010000	0,1429	0,741801
Lack of Fit	0,45306	1	0,453060	6,4723	0,125966
Pure Error	0,14000	2	0,070000		
Total SS	10,35714	6			

\* Significant Factor

TABLE 3 ESTIMATED EFFECTS MATRIX FOR THE CRYSTALLINITY DEGREE

	Effect	Std. Err.	t(3)	P	-95% Cnf. Limt.	+95% Cnf. Limt.
*Mean/Interac.	32,43365	0,101332	320,0741	0,000010	31,99766	32,86965
Mass Flow	0,37274	0,259803	1,4347	0,287830	-0,74511	1,49058
*Mold Temperature	3,10000	0,264575	11,7169	0,007205	1,96163	4,23837
1 by 2	-0,10000	0,264575	-0,3780	0,741801	-1,23837	1,03837

\* Significant Factor

With higher mold temperature, the gradient of temperature between the molten composite and the mold is smaller, and smaller cooling rates are established in the polymer matrix of RHA/PP. Consequently, the polymeric matrix is cooled more slowly what facilitates the arrangement of polypropylene molecules in the polymer phase, providing so, higher crystallinity degree.

According to the results of the estimated effect matrix it is possible to determine the statistical equation that relates the crystallinity degree with the significant statistical factors, what can be represented by Equation (1). The graphical representation of the Equation (2), Fig. 3, shows the tendency for the values of the crystallinity degree of the composite according to the processing parameter mold temperature.

$$X_C(T) = (32.43365 \pm 0.10133) + (1.55000 \pm 0.13229) \cdot T \quad (1)$$

Where  $X_c$  is the crystallinity degree and  $T$  the mold temperature.

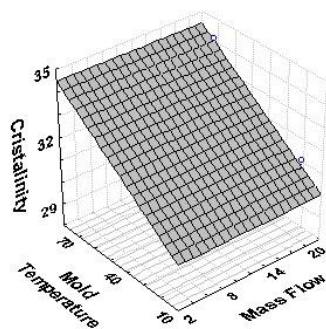


Fig. 3 Crystallinity degree as a function of mold temperature

Fig. 4 shows diagrams of stress versus strain obtained with a constant mass flow and with different mold temperatures. Diagrams represented in Fig. 4 were obtained from samples produced using mass flow equal to 4.0 g/s and mold temperatures equal to 18.0 °C and 69.0 °C. Results show higher rigidity for the samples prepared with higher mold temperature. The average values for the modulus of elasticity are  $(1539 \pm 164)$  MPa and  $(1729 \pm 157)$  MPa and the average values for the maximum strain are  $(21.6 \pm 0.4)$  MPa and  $(22.6 \pm 0.3)$  MPa for the samples of RHA/PP produced with mold temperatures equal to 18.0 °C and 69.0 °C respectively.

Fig. 5 shows typical diagrams of stress versus strain for the samples of RHA/PP produced with equal mold temperatures and different mass flows. The diagrams shown were obtained with mold temperature equal to 18.0 °C and mass flow of 4.0 g/s and 21.0 g/s. The average values for the modulus of elasticity are  $(1539 \pm 164)$  MPa and  $(1729 \pm 157)$  MPa and for the maximum strain are equal to  $(21.6 \pm 0.4)$  MPa and  $(22.6 \pm 0.3)$  MPa for the samples of RHA/PP produced with mass flow of 4.0 g/s and 21.0 g/s, respectively.

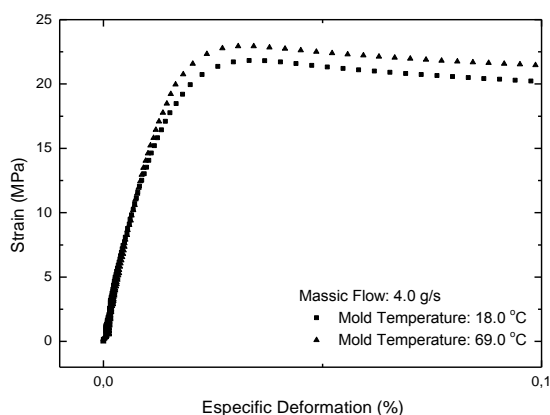


Fig. 4 Diagrams strain versus specific deformation obtained for the samples produced with mass flow equal to 4.0 g/s and mold temperature equal to 18.0 °C and 69.0 °C

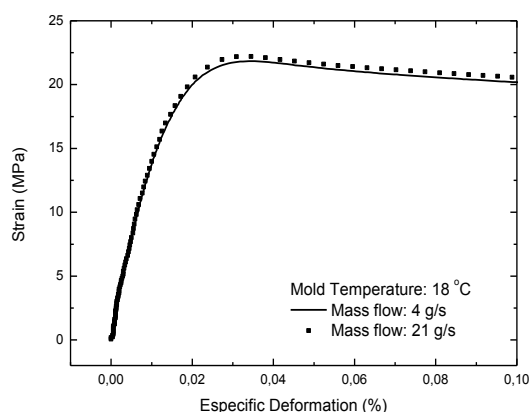


Fig. 5 Diagrams strain versus specific deformation obtained for the samples produced with mold temperature of 18.0 °C and mass flow equal to 4.0 and 21.0 g/s

Table 4 shows the results of maximum strain and modulus of elasticity for the samples RHA/PP composite injected with different mass flow and different mold temperature. From the analysis of variance (ANOVA), showed in the Tables 5 and 6, it is possible to conclude that the mass flow and the mold temperature are statistical significant factors just for the maximum strain in a reliability level of 95.0%. The modulus of elasticity does not present significance for the studied variables, so the estimated effects matrix is not necessary.

TABLE 4 MATRIX OF RESPONSE FOR THE MAXIMUM STRAIN AND MODULUS OF ELASTICITY FOR THE SAMPLES PRODUCED WITH DIFFERENT MASS FLOW AND DIFFERENT MOLD TEMPERATURE

<i>Experiment</i>	<i>Mass flow [g/s]</i>	<i>Mold Temperature [°C]</i>	<i>Maximum Strain [MPa]</i>	<i>Modulus of elasticity (MPa)</i>
1	4.0	18.0	21.6 ± 0.4	1539 ± 164
2	21.0	69.0	22.9 ± 0.2	1613 ± 243
3	21.0	18.0	22.5 ± 0.4	1437 ± 95
4	4.0	69.0	22.6 ± 0.3	1729 ± 157
5	15.0	43.5	23.1 ± 0.4	1493 ± 147
6	15.0	43.5	22.8 ± 0.4	1424 ± 85
7	15.0	43.5	23.0 ± 0.1	1410 ± 123

TABLE 5 ANOVA FOR THE MAXIMUM STRAIN

	<b>SS</b>	<b>df</b>	<b>MS</b>	<b>F</b>	<b>P</b>
<b>* Mass Flow</b>	0.532109	1	0.532109	22.80469	0.041162
<b>*Mold Temperature</b>	0.490000	1	0.490000	21.00000	0.044467
<b>1 by 2</b>	0.090000	1	0.090000	3.85714	0.188497
<b>Lack of Fit</b>	0.378367	1	0.378367	16.21572	0.056493
<b>Pure Error</b>	0.046667	2	0.023333		
<b>Total SS</b>	1.537143	6			

\* Significant Factor

TABLE 6 ANOVA FOR THE MODULUS OF ELASTICITY

	<b>SS</b>	<b>df</b>	<b>MS</b>	<b>F</b>	<b>P</b>
<b>Mass Flow</b>	19878.21	1	19878.21	10.06832	0.086612
<b>Mold Temperature</b>	33489.00	1	33489.00	16.96218	0.054206
<b>1 by 2</b>	49.00	1	49.00	0.02482	0.889288
<b>Lack of Fit</b>	24256.55	1	24256.55	12.28595	0.072637
<b>Pure Error</b>	3948.67	2	1974.33		
<b>Total SS</b>	81621.43	6			

\* Significant Factor

The estimate effects matrix, Table 7, for the maximum strain results indicates a positive effect of mold temperature and mass flow of  $(0.70000 \pm 0.71630)$  °C and  $(0.152753 \pm 0.149997)$  g/s, respectively.

TABLE 7 ESTIMATED EFFECTS MATRIX FOR THE MAXIMUM STRAIN

	<b>Effect</b>	<b>Std. Err.</b>	<b>t(3)</b>	<b>p</b>	<b>-95% Cnf. Limt.</b>	<b>+95% Cnf. Limt.</b>
<b>*Mean/Interce.</b>	22.59771	0.058504	386.2600	0.000007	22.34599	22.84943
<b>*Mass flow</b>	0.71630	0.149997	4.7754	0.041162	0.07091	1.36169
<b>*Mold Temperature</b>	0.70000	0.152753	4.5826	0.044467	0.04276	1.35724
<b>1 by 2</b>	-0.30000	0.152753	-1.9640	0.188497	-0.95724	0.35724

\* Significant Factor

The increase of the maximum strain with the mold temperature is due to the increase in the crystallinity degree established in the polymeric phase of the composite under conditions of lower cooling rate. Hot molds provide lower cooling kinetics conditions and consequently a greater number of organized molecules in the polymeric matrix of RHA/PP. As the tensile strength property of the RHA/PP composite is mainly dependent on the mechanical property of the polymeric matrix, the tensile strength of the composite will be higher.

In turn, the results indicate that the tensile strength of RHA/PP depends positively on the mass flow. The increase in the mass flow provides the filling of the mold in lower time and with highest injection pressure, which results in the forced alignment of the polypropylene molecules in the polymeric matrix of the composite. So, the injected composite solidify with the polymeric matrix oriented by the mass flow and with higher packing factor. These conditions favor the formation of a polymeric matrix with lower molecular distances and promote the increase of maximum strain. Still, the injection in conditions of higher flow favors the compression of the polymeric matrix and the interaction of the particles of rice husk ash with the molecules of polypropylene matrix and the formation of smaller amounts of voids or gaps.

In this way, these conditions favor the increase of maximum strain properties of RHA/PP. However, although the orientation takes place and the compression of the molecules of polymeric matrix increases in the mass flow, this effect was not significant for the crystallinity degree of the composite.

According to the results analyzed by the estimated effects matrix the statistical equation that relates the maximum strain with mold temperature and mass flow can be represented by the Equation (2).

$$\sigma_T(f, T) = (22.59771 \pm 0.05850) + (0.358150 \pm 0.074998) \cdot \phi_{inj} + (0.350000 \pm 0.076376) \cdot T \quad (2)$$

Where  $\sigma_T$  is the maximum strain,  $\phi_{inj}$  is the mass flow and  $T$  is the mold temperature.

The graphical representation of Equation (2), Fig. 6, illustrates the tendency for the values of maximum strain as a function of the processing parameters – mold temperature and mass flow.

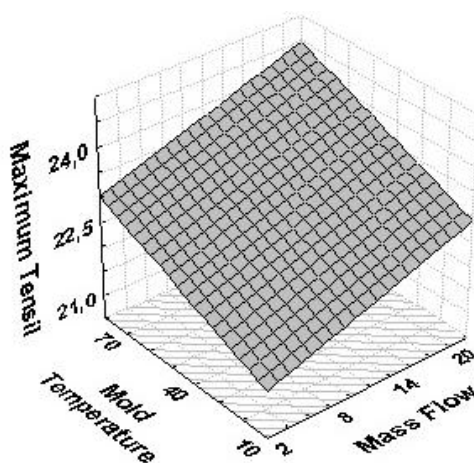


Fig. 6 Maximum strain as a function of the mold temperature and the mass flow

Table 8 shows the results for the maximum strain and flexural modulus. The results indicate that the increase in the mold temperature and in the mass flow promotes the increase of maximum strain and also the flexural modulus. The variance analysis (ANOVA) showed in Tables 9 and 10 show that these factors are significant in a reliability level of 95.0%.

TABLE 8 MATRIX OF RESPONSES FOR THE MAXIMUM STRAIN AND FLEXURAL MODULUS

Experiment	Mass Flow [g/s]	Mold Temperature [°C]	Maximum Strain [MPa]	Flexural Modulus (MPa)
1	4.0	18.0	1668 ±39	35.7 ±0.4
2	21.0	69.0	1918 ±53	36.9 ±0.2
3	21.0	18.0	1744 ±22	36.2 ±0.5
4	4.0	69.0	1895 ±23	36.7 ±0.1
5	15.0	43.5	1839 ±35	36.7 ±0.4
6	15.0	43.5	1827 ±29	36.7 ±0.4
7	15.0	43.5	1851 ±25	36.6 ±0.2

TABLE 9 ANOVA FOR THE RESULTS OF MAXIMUM STRAIN

	SS	df	MS	F	P
* Mass Flow	3216,54	1	3216,54	22,3371	0,041970
*Mold Temperature	40200,25	1	40200,25	279,1684	0,003563
1 by 2	702,25	1	702,25	4,8767	0,157881
Lack of Fit	1072,39	1	1072,39	7,4471	0,112140
Pure Error	288,00	2	144,00		
Total SS	45479,43	6			

\* Significant Factor

TABLE 10 ANOVA FOR THE RESULTS OF FLEXURAL MODULUS

	SS	df	MS	F	P
* Mass Flow	0,172965	1	0,172965	51,8894	0,018732
*Mold Temperature	0,722500	1	0,722500	216,7500	0,004582
1 by 2	0,022500	1	0,022500	6,7500	0,121690
*Lack of Fit	0,095369	1	0,095369	28,6106	0,033220
Pure Error	0,006667	2	0,003333		
Total SS	1,020000	6			

\* Significant Factor

From the results showed in the estimated effects matrix, Tables 11 and 12, it is possible to conclude that the mold temperature and mass flow have positive effects. For the bending stress the value for the mass flow is  $(55.69200 \pm 11.78356)$  g/s and for mold temperature is  $(200.50000 \pm 12.00000)$  °C. For the flexural modulus the effect of the mass flow is  $(0.40839 \pm 0.056694)$  g/s and  $(0.85000 \pm 0.057735)$  °C for the mold temperature.

TABLE 11 ESTIMATED EFFECTS MATRIX FOR THE RESULTS OF MAXIMUM BENDING STRESS

	Effect	Std. Err.	t(3)	P	-95% Cnf. Limit.	+95% Cnf. Limit.
*Mean/Interec.	1816,776	4,59597	395,2972	0,000006	1797,001	1836,551
* Mass Flow	55,692	11,78356	4,7262	0,041970	4,991	106,392
*Mold Temperature	200,500	12,00000	16,7083	0,003563	148,868	252,132
1 by 2	-26,500	12,00000	-2,2083	0,157881	-78,132	25,132

\* Significant Factor

TABLE 12 ESTIMATED EFFECTS MATRIX FOR THE RESULTS OF FLEXURAL MODULUS

	Effect	Std. Err.	t(3)	P	-95% Cnf. Limit.	+95% Cnf. Limit.
*Mean/Interec.	36,47426	0,022112	1649,494	0,000000	36,37912	36,56940
* Mass Flow	0,40839	0,056694	7,203	0,018732	0,16446	0,65232
*Mold Temperature	0,85000	0,057735	14,722	0,004582	0,60159	1,09841
1 by 2	-0,15000	0,057735	-2,598	0,121690	-0,39841	0,09841

\* Significant Factor

According to the statistical analysis obtained by the estimated effects matrix it is possible to determine the statistical equations that relate the maximum bending stress and the flexural modulus with the mold temperature and mass flow, showed in Equations (3) and (4), respectively.

$$\sigma_F(f, T) = (1816, 776 \pm 4.59597) + (27.846 \pm 5.89178) \cdot \phi_{inj} + (100.250 \pm 6.0000) \cdot T \quad (3)$$

$$E_F(f, T) = (36.47426 \pm 0.022112) + (0.204195 \pm 0.028347) \cdot \phi_{inj} + (0.425 \pm 0.0288675) \cdot T \quad (4)$$

Where  $\sigma_{MAX}$  is the maximum strain,  $\sigma_{ESC}$  is the yielding stress,  $\phi_{inj}$  is mass flow and  $T$  is the mold temperature.

The graphic representation of Equations (3) and (4), showed in Figs. 7 and 8 respectively, illustrates the tendency for the values of maximum strain and yielding stress as a function of the injection processing parameters, mold temperature and mass flow.

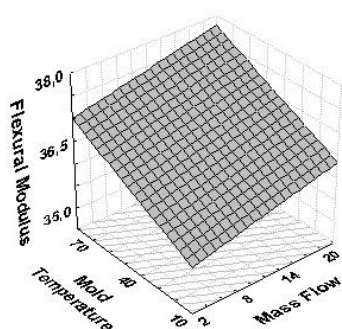


Fig. 7 Maximum bending stress as a function of mold temperature

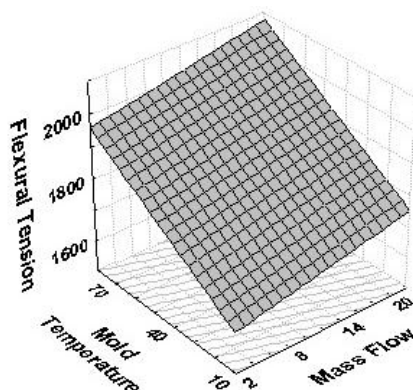


Fig. 8 Maximum bending stress as a function of mass flow

Fig. 9 shows the images of scanning electron microscopy for the samples of RHA/PP composite produced with mass flow of 4.0 g/s and mold temperature of 69.0°C. The images present particles of RHA of different sizes dispersed in the polypropylene matrix as well as many defects propagated from RHA due to the incompatibility between the polymeric matrix

and RHA particles, Fig. 9 shows the interface of low compatibility between the matrix of polypropylene and one particle of RHA.

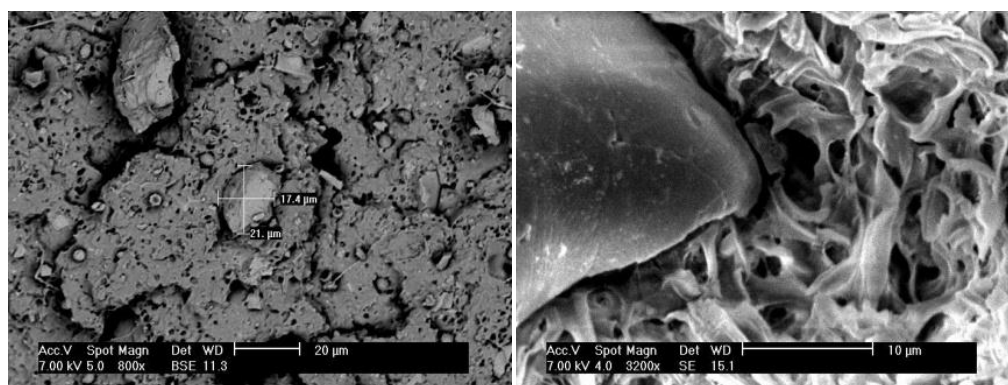


Fig. 9 Images of Scanning Electron Microscopy for the samples of RHA/PP produced with mass flow of 4.0 g/s and mold temperature of 69.0°C

The micrographs indicate the need of use of compatibilizer agents to improve the mechanical properties of the RHA/PP composite. Although the particles of rice husk ash are distributed homogeneously, there are many faults in the interface between the particles and the polymeric matrix. These characteristics affect the mechanical properties of the composite.

#### IV. CONCLUSIONS

This work shows the importance of the injection processing parameters in the mechanical properties of RHA/PP composites as a function of the crystallinity degree of the polymeric matrix.

The mold temperature is a meaningful factor in the determination of crystallinity degree in the polypropylene matrix. The increase in the mold temperature provides smaller temperature gradients in the polymeric matrix of PP and slower cooling. These kinetics conditions of cooling provide an increase in the crystallinity degree of CCA/PP.

Both mold temperature and mass flow are meaningful factors in the tensile and bending properties. The increase in the mold temperature and in the mass flow provides better properties of tensile strength and bending and so, a better rigidity of the composite CCA/PP. These effects are associated with the increase in the crystallinity degree and also with the packing factor of the polypropylene matrix of the composite.

#### ACKNOWLEDGEMENTS

The researches thank the Laboratory of Advanced Materials and Polymer Processing from UNESC, the Laboratory of Materials from SENAI/CTCMat and the Program of Post-Graduation in Chemical Engineering of UFSC.

#### REFERENCES

- [1] Louis, N. S. M. and S. Tomas. *Effect of rice husk ash on the mechanical properties of low density polyethylene*. Journal Of Scientific & Industrial Research, vol. 72, pp. 441-445, 2013.
- [2] M. F. M. Zain, M. N. Islam, F. Mahmud, and M. Jamil. *Production of rice husk ash for use in concrete as a supplementary cementitious material*. Construction and Building Materials, vol. 25, pp. 798-805, 2011.
- [3] Hwang Chao-Lung, Bui Le Anh-Tuan, and Chen Chun-Tsun. *Effect of rice husk ash on the strength and durability characteristics of concrete*. Construction and Building Materials, vol. 25, pp. 3768-3772, 2011.
- [4] M. H. Zhang, R. Lastra and V. M. Malhotra. *Rice-husk ash paste and concrete: some aspects of hydration and the microstructure of the interfacial zone between the aggregate and paste*. Cement and Concrete Research, vol. 26, iss. 6, pp. 963-977, 1996.
- [5] S. N. Raman, T. Ngo, P. Mendis, and H. B. Mahmud. *High-strength rice husk ash concrete incorporating quarry dust as a partial substitute for sand*. Construction and Building Materials, vol. 25, pp. 3123-3130, 2011.
- [6] M. Nehdi, J. Duquette, and A. El Damatty. *Performance of rice husk ash produced using a new technology as a mineral admixture in concrete*. Cement and Concrete Research, vol. 33, pp. 1203-1210, 2003.
- [7] M. Ghorbani, M. S. Lashkenari, and H. Eisazadeh. *Application of polyaniline nanocomposite coated on rice husk ash for removal of Hg (II) from aqueous media*. Synthetic Metals, vol. 161, pp. 1430-1433, 2011.
- [8] V. C. Srivastava, I. D. Mall, and I. M. Mishra. *Characterization of mesoporous rice husk ash (RHA) and adsorption kinetics of metal ions from aqueous solution onto RHA*. Journal of Hazardous Materials B, vol. 134, pp. 257-267, 2006.
- [9] I. Dahlan, K. T. Lee, A. H. Kamaruddin, and A. R. Mohamed. *Sorption of SO<sub>2</sub> and NO from simulated flue gas over rice husk ash (RHA)/CaO/CeO<sub>2</sub> sorbent: Evaluation of deactivation kinetic parameters*. Journal of Hazardous Materials, vol. 185, pp. 1609-1613, 2011.
- [10] I. Dahlan, K. T. Lee, A. H. Kamaruddin, and A. R. Mohamed. *Selection of metal oxides in the preparation of rice husk ash (RHA)/CaO sorbent for simultaneous SO<sub>2</sub> and NO removal*. Journal of Hazardous Materials, vol. 166, pp. 1556-1559, 2009.



- [11] H. T. Jang, Y. Park, Y. S. Ko, and J. Y. Lee, Bhagiyalakshmi Margandan. *Highly siliceous MCM-48 from rice husk ash for CO<sub>2</sub> adsorption*. International Journal of Greenhouse Gas Control, vol. 3, pp. 545-549, 2009.
- [12] M. C. Manique, C. S. Faccini, B. Onorevoli, E. V. Benvenuti, and E. B. Caramão. *Rice husk ash as an adsorbent for purifying biodiesel from waste frying oil*. Fuel, vol. 92, pp. 56-61, 2012.
- [13] S. Detphan and P. Chindaprasirt. *Preparation of fly ash and rice husk ash geopolymer*. International Journal of Minerals, Metallurgy and Materials, vol. 16, iss. 6, p. 720, December 2009.
- [14] A. Nazari, A. Bagheri, and S. Riahi. *Properties of geopolymer with seeded fly ash and rice husk bark ash*. Materials Science and Engineering, vol. 528, pp. 7395-7401, 2011.
- [15] F. Bondioli, F. Andreola, L. Barbieri, T. Manfredini, and A. M. Ferrari. *Effect of rice husk ash (RHA) in the synthesis of (Pr, Zr) SiO<sub>4</sub> ceramic pigment*. Journal of the European Ceramic Society, vol. 27, pp. 3483-3488, 2007.
- [16] L. Sereda, M. M. López-González, L. L. Y. Visconte, R. C. di, R. Nunes, C. R. G. Furtado and E. Riande. *Influence of silica and black rice husk ash fillers on the diffusivity and solubility of gases in silicone rubbers*. Polymer, vol. 44, pp. 3085-3093, 2003.
- [17] H. Ismail, M. N. Nasaruddin, and H. D. Rozman. *The effect of multifunctional additive in white rice husk ash filled natural rubber compounds*. European Polymer Journal, vol. 35, pp. 1429-1437, 1999.
- [18] H. Ismail, M. N. Nasaruddin, U. S. Ishaku. *White rice husk ash filled natural rubber compounds: the effect of multifunctional additive and silane coupling agents*. Polymer Testing 18 (1999) 287-298.
- [19] D. García, J. López, R. Balart, R. A. Ruseckaite, P. M. Stefani. *Composites based on sintering rice husk-waste tire rubber mixtures*. Materials and Design 28 (2007) 2234-2238.
- [20] N. Chand, P. Sharma, and M. Fahim. *Tribology of maleic anhydride modified rice-husk filled polyvinylchloride*. Advanced Materials and Processes Research Institute (AMPRI), CSIR, Hoshangabad. Wear, vol. 269, pp. 847-853, 2010.
- [21] S. Siriwardena, and H. Ismail, U. S. *Effect of mixing sequence in the preparation of white rice husk ash filled polypropylene/ethylene-propylene-diene monomer blend* Polymer Testing, vol. 20, pp. 105-113, 2001.
- [22] H. Ismail, J. M. Nizam, and H. P. S. A. Khalil. *The effect of a compatibilizer on the mechanical properties and mass swell of white rice husk ash filled natural rubber/linear low density polyethylene blends*. Polymer Testing, vol. 20, pp. 125-133, 2001.
- [23] M. Y. A. Fuad, I. Yaakob, Z. A. Mohd Ishak, and A. K. Mohd Omar. *Density Measurement of Rice Husk Ash Filler Particles in Polypropylene Composites*. Polymer Testing, vol. 12, pp. 107-112, 1993.
- [24] M. Y. A. Fuad, Z. Ismail, Z. A. M. Ishak and A. K. M. Omar. *Application of Rice Husk Ash as Fillers in Polypropylene: Effect of Titanate, Zirconate and Silane Coupling Agents*. Plastics Technology Group, Standards and Industrial Research Institute of Malaysia (SIRIM), Eur. Polym. J. vol. 31, iss. 9, pp. 885-893, 1995.
- [25] H. Yang, H. Kim, J. Son, H. Park, B. Lee, and T. Hwang. *Rice-husk flour filled polypropylene composites; mechanical and morphological study*. Composite Structures, vol. 63, pp. 305-312, 2004.
- [26] H. Yang, H. Kim, H. Park, B. Lee, and T. Hwang. *Effect of compatibilizing agents on rice-husk flour reinforced polypropylene composites*. Composite Structures, vol. 77, pp. 45-55, 2007.
- [27] A. Nourbakhsha, F. F. Baghlanib, and A. Ashoric. *Nano-SiO<sub>2</sub> filled rice husk/polypropylene composites: Physico-mechanical properties*. Industrial Crops and Products, vol. 33, pp. 183-187, 2011.
- [28] H. G. B. Premalal, H. Ismail, and A. Baharin. *Comparison of the mechanical properties of rice husk powder filled polypropylene composites with talc filled polypropylene composites*. Polymer Testing, vol. 21, pp. 833-839, 2002.
- [29] G. C. Nascimento et al. *Effect of Different Concentrations and Sizes of Particles of Rice Husk Ash - RHS in the Mechanical Properties of Polypropylene*. Materials Science Forum, vol. 660-661, pp. 23-28, 2010.